Supplementary data

Synergistic actions of phytonutrients capped nanosilver as a novel broad-spectrum antimicrobial agent: Unveiling the antibacterial effectiveness and bactericidal mechanism.

Kavya Moorthy[a], Kai-Chih Chang[b,c], Po-Jen Yu[b], Wen-Jui Wu[b], Mei-Yi Liao[d], Hsiao-Chi Huang[b], Hsiang-Chi Chien[d], Cheng-Kang Chiang [a,]*

[a] Department of Chemistry, National Dong Hwa University, Shoufeng, Hualien, Taiwan, 974301

[b] Department of Laboratory Medicine and Biotechnology, Tzu Chi University, Hualien, Taiwan, 97004

[c] Department of Laboratory Medicine, Buddhist Tzu Chi General Hospital, Hualien, Taiwan, 97004

[d] Department of Applied Chemistry, National Pingtung University, Pingtung, Taiwan, 900393

*To whom correspondence should be addressed, e-mail: ckchiang@gms.ndhu.edu.tw

Tel.: +886-3-8903622; Fax: +886-3-8900162

Table of Contents   S2

I. Experimental Section   S4

I. Experimental Section

1. Preparation of aqueous cogon grass extracts

To compare the reducing ability of cogon grass extract for the synthesis of CGE-mediated AgNPs, three extraction methods, including decoction, fresh leaves extraction, and sonication extraction were performed. Aqueous decoction extract of cogon grass was prepared by boiling the solution comprised of 1g of dry plant material with 50 mL DI at 70 ºC for 30 min under magnetic stirring. To prepare fresh CG leaves extraction, 1 g of chopped fresh CG leaves was aged with 50 mL DI and blended with a blender for 3 min at room temperature (RT). A modified sonication method was adopted to prepare aqueous sonicated CGE by using 1 g of dry cogon grass power with 50 mL of DI using an ultrasonicator bath (Branson Ultrasonic, Brookfield, Connecticut, USA) for 50 min at RT. All the extracts were filtered through Whatman No.1 filter paper and kept at 4 ºC before use.

2. Total phenolic assay and Total flavonoid assay of CGEs

5 mL of the as-prepared cogon grass extract, including A-DE-, A-BL-, E-DE-, and E-BL-CGE was dried using a speed vac for 6 hr, respectively. 2 mg of each extract pellet was dissolved in 1 mL of methanol and sonicated for 45 min at RT. After centrifugation at 1000 g for 10 min, the clear supernatant was collected and stored for the following assay analysis. The total phenolic content (TPC) was determined by the Folin-Ciocalteu assay[1, 2]. An aliquot (0.08 mL) of CG extracts and standard gallic acid solution (5- 500 µg/mL) were mixed with DI (0.24 mL) and 0.08 mL of Folin-Ciocalteu's phenol reagent, respectively. After 5 min incubation, 0.4 mL of saturated sodium carbonate solution (8 % w/v in water) was added and the volume was made up to 1.2 mL with DI. After incubation for 30 min in

the dark at RT, the absorbance at 765 nm was recorded. TPC value for each CGE was expressed as mg Gallic acid equivalents (GAE)/g of dry plant material.

The total flavonoid content (TFC) was measured by the aluminum chloride ($AlCl_3$) colorimetric assay. An aliquot (0.5 mL) of extracts or standard solutions of quercetin (5-250 µg/mL) was mixed with 0.5 mL of 2 % $AlCl_3$ solution. After incubated for 60 min at RT, the absorbance at 430 nm was measured. TFC value was expressed as mg quercetin equivalents (QE)/g of dry plant material.[3]

3. *DPPH free radical scavenging assay*

The DPPH free radical scavenging assay for the AgNPs was performed according to a reported method with some modifications [4]. An aliquot of 200 µL of various concentrations of CGE-mediated AgNPs (125, 250, and 500 µg/mL) in ethanol was mixed with 200 µL of 0.04% (w/v) DPPH in ethanol solution and kept in the dark for 30 min at RT. The absorbance was measured at 521 nm against a control group of 0.02% DPPH ethanolic solution. The DPPH free radical scavenging activity was calculated using the following equation.

DPPH scavenging effect (%) = $[(A_0 - A_t)/A_0] \times 100\%$

While A_0 and A_t are the absorbance of the control and the analyte, respectively.

4. *Detection of Ag ions released from CGE-AgNPs*

200 ppm A-DE- and A-BL-AgNPs were first resuspended in deionized water. After incubation for 0.5, 1, 3, 6, and 24 h, 5 mL of the CGE-AgNPs solution was collected and subsequently centrifuged at 15,000 g for 20 min. The supernatant solutions were harvested

and diluted with nitric acid (5M) to measure Ag^+ concentrations and measured in triplicates (n=3) through the atomic absorption spectrophotometry (AAS)[5]

5. *Minimum inhibitory concentration and zone of inhibition test*

The zone of inhibition test was done against three bacterial strains, including *Escherichia coli* (*E. coli*)*, Pseudomonas aeruginosa* (*P. aeruginosa*), and *Staphylococcus aureus* (*S. aureus*) using the standard disc diffusion method[6, 7] The new bacterial culture was cultured in Luria-Bertani medium (LB broth). Three above-mentioned bacterial strains were separately swabbed onto the LB agar plates with the help of sterile cotton swabs. 10 μL of CGE-mediated AgNPs solution (4 mg/mL) was poured onto the dishes. After incubation at 37 ℃ for 24 h, a diameter of zone of inhibition for CGE mediated AgNPs against three tested bacteria was measured. Colistin was used as a positive control in this study.

The antibacterial activities of the biosynthesized AgNPs were tested in triplicates using the micro-broth dilution method to determine the minimum inhibitory concentration (MIC) values against bacteria. Three non-drug resistant Gram-negative and one Gram-positive bacteria, such as *E. coli*, *P. aeruginosa*, *A. baumannii*, and *S. aureus*, as well as drug-resistant bacteria, including colistin- and imipenem-resistant *A. baumannii,* were selected, respectively. Various concentrations of CGE-mediated AgNPs (1-64 μg/mL, 100 μL) were incorporated with 100 μL of tested strains of bacteria (10^6 CFU/mL) in Mueller-Hinton broth (MH broth) at each well of the 96-well microplate and incubate at 37 ℃ for 18 h. The MIC value is defined as the lowest concentration of NPs where no visible bacterial growth is observed or measured spectrophotometrically at 600 nm. Gallic acid-mediated AgNPs were prepared following the previously reported control[8].

6. Time-dynamic antibacterial test

The antimicrobial activity of A-BL-AgNPs was evaluated using a time-dynamic antibacterial assay at various incubation times. *E. coli* and *S. aureus* cells (10^7 CFU/mL) were respectively treated with 8 or 16 µg/mL of A-BL-AgNPs in phosphate-buffered saline (PBS) buffer. In the absence of A-BL-AgNPs, a bacterial control group of *E. coli* and *S. aureus* was cultured. To assess the survival rate (%) at each time point, bacteria were taken from 0 to 4 h, diluted, and cultivated on LB plates[9] (n=3).

7. Reactive oxygen species measurement

Reactive oxygen species (ROS) were measured for the bio-synthesized AgNPs according to previously reported literature with slight modification [10, 11]. Briefly, *E. coli* ($5×10^7$ CFU/mL) were first incubated with 80 µg CGE-mediated AgNPs for 2 h. Then, the mixtures were washed twice with PBS and incubated with 25 µM 2', 7'-dichlorofluorescein-diacetate (DCFH-DA) for 30 min. After washing with PBS twice, the microscopic images were taken using an Olympus IX71 microscope (Tokyo, Japan) with a SPOT RT3 digital camera. The fluorescence images of DCFH-DA-labeled bacteria were recorded with the excitation at 510–530 nm.

8. Electron microscopy measurement

Samples containing 10^9 CFU/mL of *E. coli* in MH broth were incubated with CGE-mediated AgNPs (20 µg) at 37 °C for 30 min. The bacterial cells were added with phosphate-buffered saline (PBS, pH 7.4) as control cells in the study. The treated cells were fixed using 2.5% (w/v) glutaraldehyde in 0.1 M cacodylate buffer and 1% tannic acid at 4 °C for 1 h and washed twice with DI and PBS, prior to dehydrating using anhydrous ethanol. After drying and coating with gold, bacterial cells were observed using the Hitachi S-4700

scanning electron microscope (Tokyo, Japan). To further capture the transmission electron microscopy images of bio-synthesized AgNPs treated with *E. coli*, a drop containing the bacteria and AgNPs was deposited onto a carbon-coated copper grid and dried in the air before examining using the H-7500 TEM)[12, 13].

9. *In-vitro Hemolysis assay*

The hemolytic activity of the CGE-mediated AgNPs toward human red blood cells (RBCs) was investigated according to a reported protocol with some modification[11, 12]. Briefly, freshly harvested RBCs were first centrifuged with 3500 *g* at 4 °C for 10 min and washed with 10 mM PBS buffer three times. Next, 500 μL of 4% erythrocyte suspension was mixed with 50 μL of AgNPs (31.25–4000 μg/mL) and incubated at 37 °C for 1 h. After centrifugation at 3500 *g* for 10 min, 200 μL of the resulting supernatant was transferred into the 96-well plate, and optical density at 600 nm was recorded. Finally, 0% and 100% lysis efficiency were determined by incubating the RBCs with 10 mM PBS and a 0.1% (v/v) Triton X-100 solution.

10. *Examination of putative phytochemicals in CGEs by high-resolution LC-MS*

Identification of potential chemical constituents in all the four types of CGEs was performed with a Shimadzu 9030 liquid chromatography coupled to a quadrupole time-of-flight mass spectrometry (LC-QTOF-MS) system with an ESI source, which was equipped with LC-30AD binary pumps, SIL-30AC auto-sampler, and CTO-20AC column heater. Both positive and negative ionization modes were performed. Instrument control and data analysis were carried out using a Shimadzu Lab solution V5.97.1 software. The chromatographic separation was performed using a Fortis C_{18} analytical column (100 mm × 2.1mm, 5 μm) as a stationary phase and maintained at 40 ºC, whereas the mobile phase

consisted of DI with 0.1 % formic acid as solvent A and methanol with 0.1% formic acid as solvent B, respectively. 5 µL of each sample was injected with a 22 min analysis time. The instrumental setting was used as below: flow rate of nebulizing gas at 3.0 L/min, heating gas at 10.0 L/min, drying gas flow at 10.0 L/min, and inference temperature of 300 C. Putative bioactive compounds in the CGEs was identified by using the Lab Solutions Insight MS library software and previously reported pieces of literature with ± 5 ppm mass error tolerance.

11. LDI-mass spectrometric analysis of bio-synthesized Ag NPs

LDI mass spectrometric spectra of purified GA-AgNPs and A-BL-AgNPs (40 µg each) were recorded by using an AXIMA Performance MALDI TOF-TOF Mass Spectrometer (Shimadzu Corporation, Kyoto, Japan), respectively. The samples were irradiated with a 337 nm nitrogen laser at 10 Hz. Ion source, lens, and linear detector voltage were set at 20.0 kV, 6.0 kV, and 2.8 kV, respectively. Mass spectra were acquired in the reflectron negative mode with 100 laser pulses from random positions on the same sample spot. Mass spectrometry was calibrated with 10 nm gold nanoparticles using the signals from the Au clusters ($[Au_n]^+$; n = 1–3).
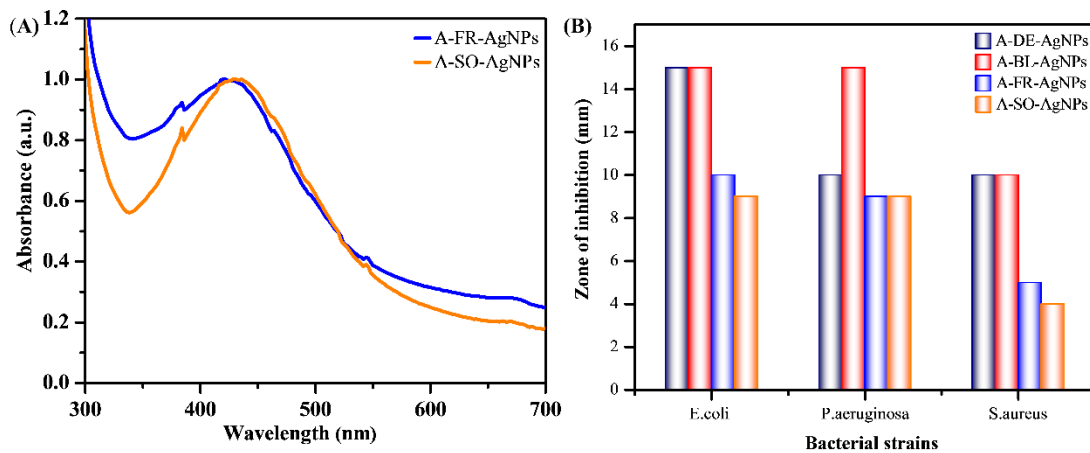
Fig. S1. (A) UV–Vis absorption spectra of A-FR-AgNPs and A-SO-AgNPs. (B) The diameter of the zone of inhibition (mm) produced by CGE-mediated AgNPs against three different bacteria.

Effect of temperature for the preparation of A-BL-AgNPs

Taking into consideration that the blended extraction method using dry CG leaves is a much more time-saving and efficient technique, the formation of AgNPs using A-BL-CGE at different reaction temperature were investigated. As shown in Fig. S2A, UV−Vis spectra of purified A-BL-AgNPs obtained at RT, 60 ℃ and 100 ℃ showed maximum absorbance at 434 nm, 436 nm, and 432 nm respectively. A visible color change occurred while the reaction temperature was set at RT for 11 hr, whereas the formation of A-BL-AgNPs at 60 ℃ and 100 ℃ was completed at 15 and 10 min, respectively. Both AgNPs were prepared at RT and 60 ℃ are stable in DI for a week, whereas A-BL-AgNPs acquired at 100 ℃ are easy to aggregate once the reaction solution was cooled down. In addition, the bar plot from the agar diffusion test (Fig. S2B) reveals that the A-BL-AgNPs synthesized at 60 ℃ possess superior antibacterial activity against all three tested bacterial strains.
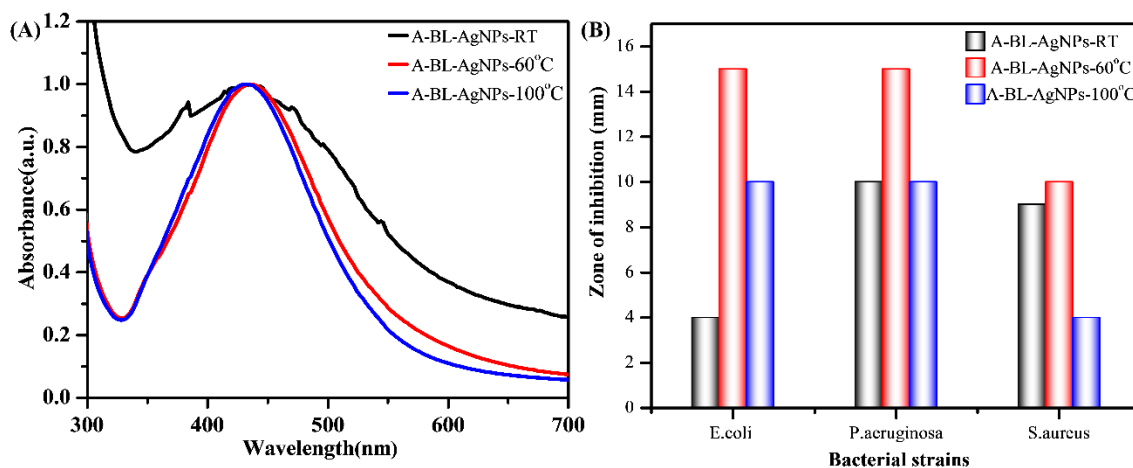
Fig. S2. (A) UV−Vis spectra and (B) Plot of inhibition zone (nm) for the A-BL-AgNPs were prepared at RT, 60 ℃, and 100 ℃, respectively.

Effect of plant material concentration for the preparation of A-BL-AgNPs

To further understand the impact of CGE concentration on the formation of AgNPs, aqueous blended CGEs were first prepared with four different dried CG powder/DI weight ratios, including 0.5 (0.5×), 1 (1×), 2 (2×), and 5 (5×) grams of dry CG leaves and 50 mL DI, respectively. A-BL-AgNPs were synthesized by mixing 10 mL of as-prepared A-BL-CGEs with 5 mM of AgNO$_3$ solution (90 mL) and incubated at 60 ºC for 15 min. These purified Ag nanomaterials were named A-BL-AgNP-0.5×, A-BL-AgNP-1×, A-BL-AgNP-2×, and A-BL-AgNP-5×, respectively.

As shown in Fig. S3A, UV−Vis spectra of purified AgNPs made from 0.5× A-BL-CGE show a characteristic peak at 432 nm, whereas A-BL-AgNP-1× and A-BL-AgNP-2× show SPR peak at 436 nm and 440 nm respectively. Besides, a broader absorption peak at 460 nm for A-BL-AgNP-5× was observed. Among these four AgNPs, A-BL-AgNP-0.5× and A-BL-AgNP-1× are well-dispersed in DI for 1 week, whereas A-BL-AgNP-2×and A-BL-AgNP-5× were aggregated as soon as the reaction solution was cooled down to RT. Besides, Fig. S3B displays that A-BL-AgNP-1× provides the maximum zone of inhibition effectiveness against *E. coli, P. aeruginosa*, and *S. aureus*, respectively.
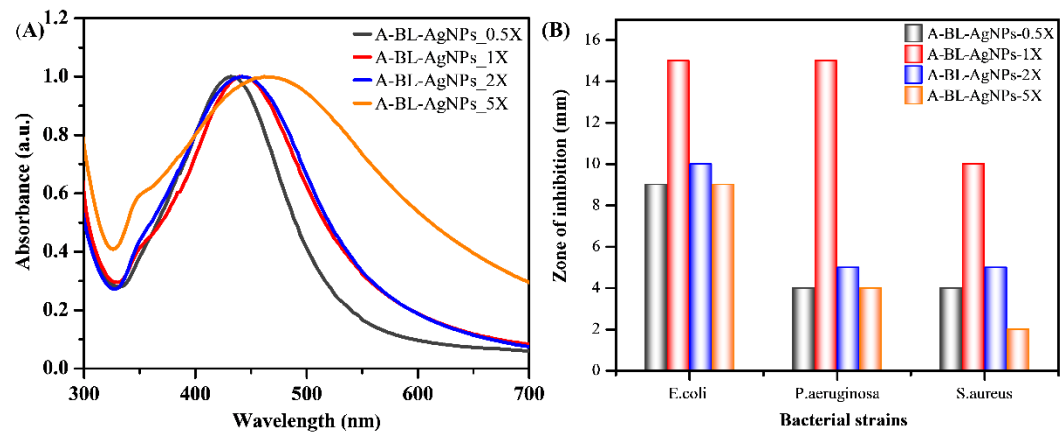
Fig. S3. (A) UV–Vis spectra and (B) The diameters of the agar diffusion test for the A-BL-AgNPs were prepared using A-BL-CGEs with different CG concentrations.
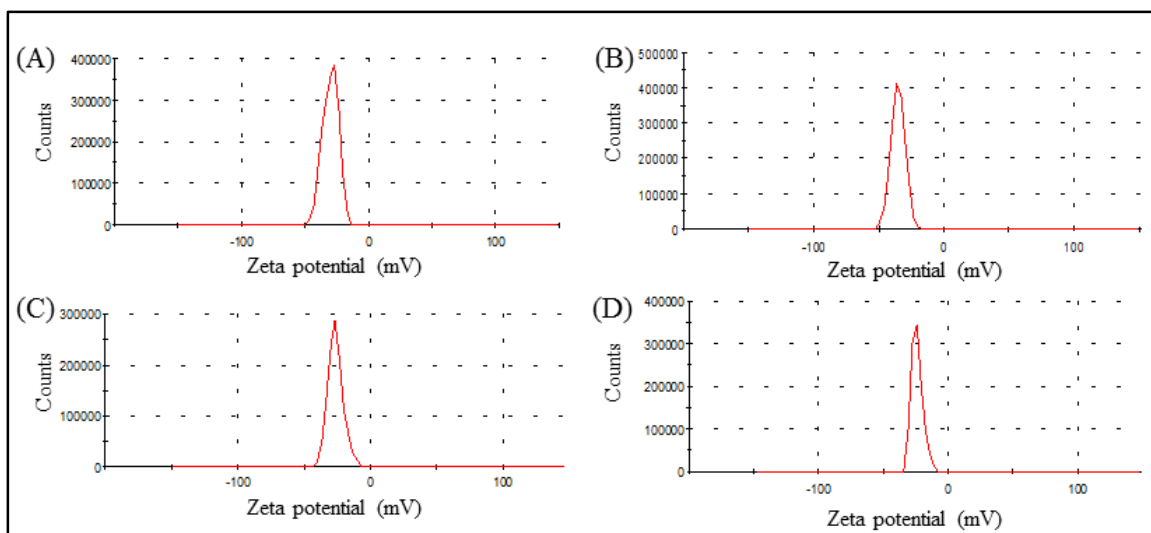
Fig. S4. Zeta potential images of (A) A-DE-AgNPs, (B) A-BL-AgNPs, (C) E-DE-AgNPs, and (D) E-BL-AgNPs.
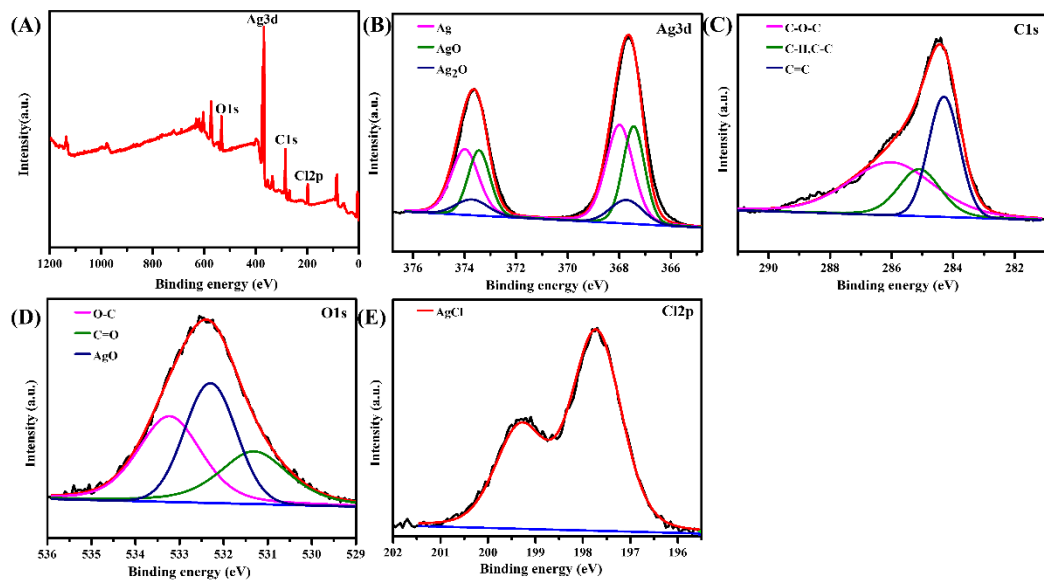
Fig. S5. (A) XPS survey spectra of A-DE-AgNPs and the deconvolution of (B) Ag 3d, (C) C 1s, (D) O 1s, and (E) Cl 2p, respectively.
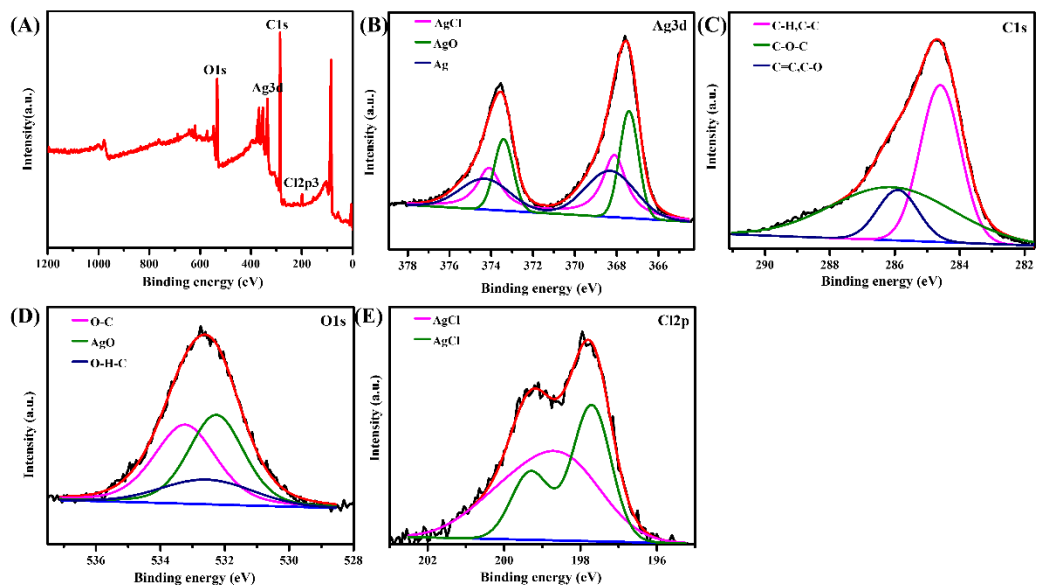
Fig. S6. (A) XPS survey spectra of E-DE-AgNPs and the deconvolution of (B) Ag 3d, (C) C 1s, (D) O 1s, and (E) Cl 2p, respectively.
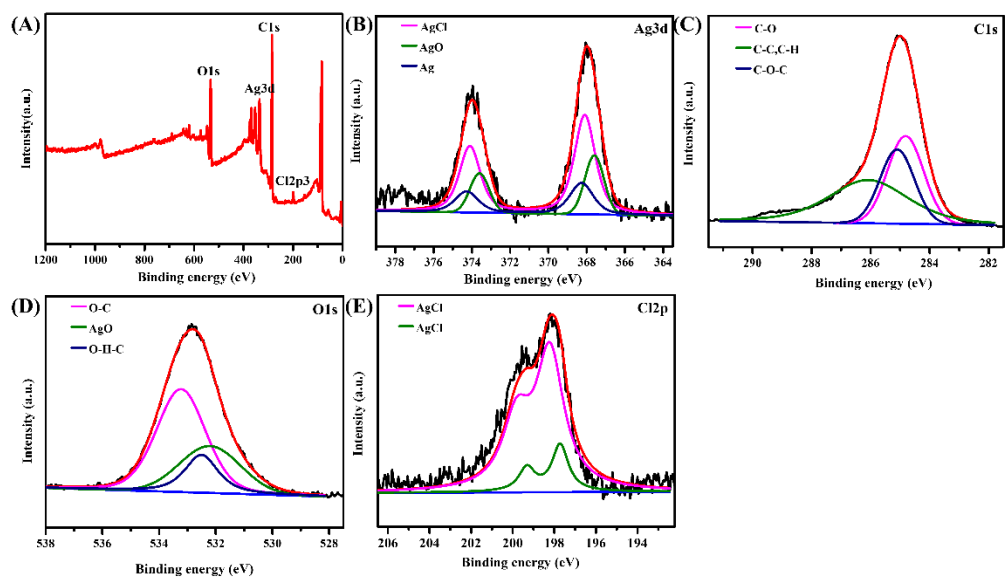
Fig. S7. (A) XPS survey spectra of E-BL-AgNPs and the deconvolution of (B) Ag 3d, (C) C 1s, (D) O 1s, and (E) Cl 2p, respectively.
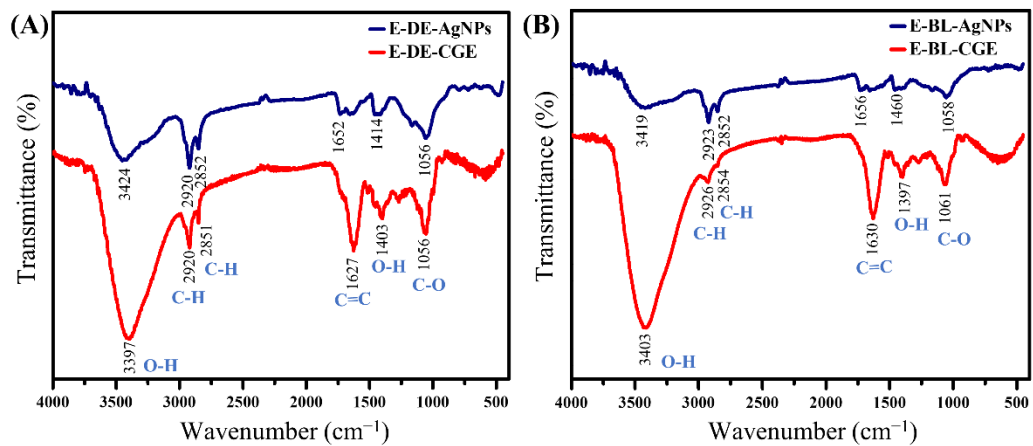
Fig. S8. FT-IR spectra of (A) E-DE-CGE and E-DE-AgNPs, (B) E-BL-CGE and E-BL-AgNPs
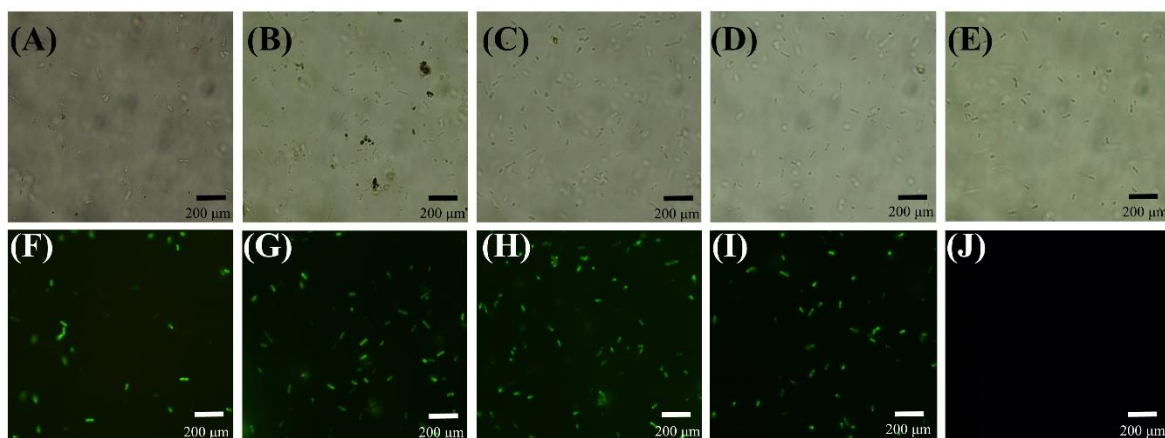
Fig. S9. (A-E) Bright-field and (F-J) fluorescence images of *E. coli* incubated with (A, F) A-DE-AgNPs, (B, G) A-BL-AgNPs, (C, H) E-DE-AgNPs, (D, I) E-BL-AgNPs, and (E, J) untreated bacteria after DCFH-DA treatment.
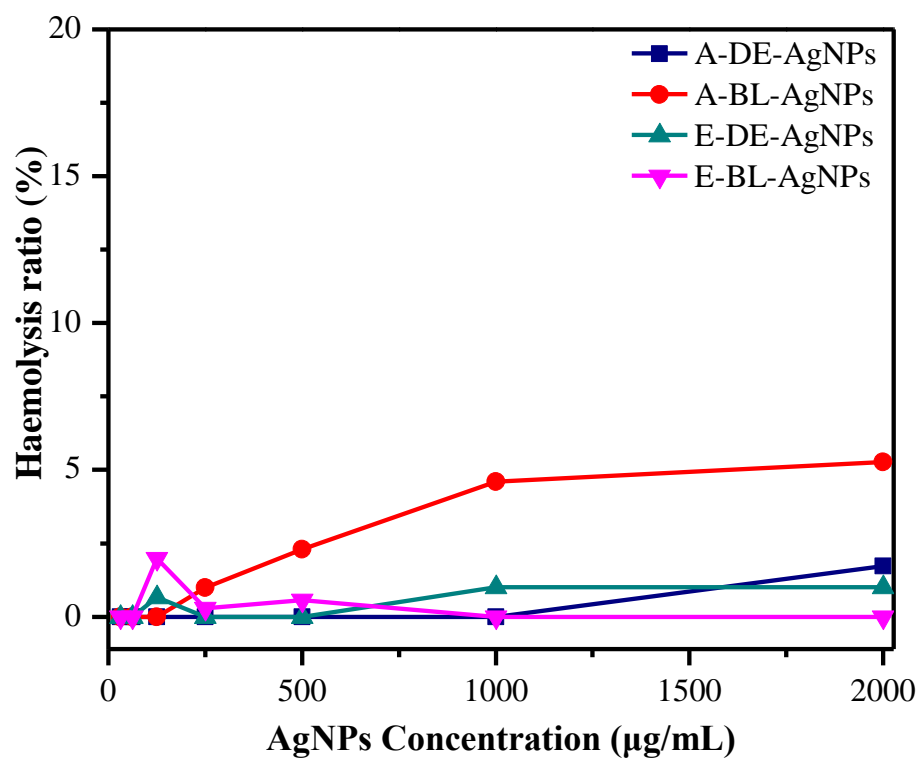
Fig. S10. Hemolytic activities of CGE mediated AgNPs against human RBCs.

Table S1. Comparison of MIC against *E. coli* strain between AgNPs synthesized using different plant extracts and our method.

Plant mediated AgNPs	Particle size (nm)	MIC (μg/mL)	Reference
Pu-erh tea	4.06	7.8	14
Murraya koenigii	5-20	16	15
Alpinia katsumadai	12.6	20	16
Lavandula intermedia	12.6	15	17
Punica granatum	15	30	18
Abelmoschus esculentus	16.9	65.5	19
Equisetum arvense	18	64	20
Vaccinium corymbosum	20	8.2	21
Cestrum nocturnum	20	8	22
Camellia Sinensis	34.68	15	23
A-BL-AgNPs	28.0 ±4.7	4	Our study
E- BL-AgNPs	20.1±5.5	16	Our study

Table S2. Positive ionization mode LC-MS analysis reveals the 20 most abundant putative phytochemicals detected in aqueous blended CGE.

No	Identified Compound	RT (min)	Exact m/z (Da)	Found m/z (Da)	Formula	Mass Error (ppm)	Ref
1	7-O-β-D-glucopyranosyl-4-metho methyl coumarin	4.96	369.1186	369.1180	$C_{17}H_{20}O_9$	-1.5	24
2	4-acetyl-2-methoxyphenol	5.85	167.0708	167.0703	$C_9H_{10}O_3$	-3.1	25
3	Impecyloside	6.18	721.2344	721.2338	$C_{34}H_{40}O_{17}$	-0.8	24
4	Chlorogenic acid	6.46	355.1029	355.1024	$C_{16}H_{18}O_9$	-1.4	26
5	p-vinyl guaiacol	6.98	151.0759	151.0754	$C_9H_{10}O_2$	-3.3	25
6	Graminone B	7.04	403.1393	403.1387	$C_{21}H_{22}O_8$	-1.5	24
7	Acetoveratrone	7.45	181.0865	181.0859	$C_{10}H_{12}O_3$	-3.1	25
8	Vanillic acid	7.69	169.0501	169.0495	$C_8H_8O_4$	-3.5	25, 26
9	1-(4-hydroxy-3,5-dimethoxyphenyl)ethanone	8.19	197.0814	197.0808	$C_{10}H_{12}O_4$	-3.0	25
10	Vanillin	8.38	153.0552	153.0546	$C_8H_8O_3$	-3.7	25, 26
11	Imperanene	9.18	331.1545	331.1540	$C_{19}H_{22}O_5$	-1.6	26
12	Ferulic acid	10.79	195.0657	195.0652	$C_{10}H_{10}O_4$	-2.7	25
13	Tabanone	11.00	191.1436	191.1430	$C_{13}H_{18}O$	-3.1	26
14	Cylindrene	12.24	233.1542	233.1536	$C_{15}H_{20}O_2$	-2.4	26
15	4'-hydroxy-5-methoxy flavone	12.66	269.0814	269.0808	$C_{16}H_{12}O_4$	-2.2	27, 28
16	2,4-di-tert-butylphenol	13.91	207.1749	207.1743	$C_{14}H_{22}O$	-2.8	25
17	Linoleic acid	14.69	281.2480	281.2475	$C_{18}H_{32}O_2$	-1.9	25
18	Simiarenol	16.06	427.3940	427.3934	$C_{30}H_{50}O$	-1.3	28
19	Caffeic acid	16.38	181.0501	181.0495	$C_9H_8O_4$	-3.2	26
20	Arundoin	18.00	441.4096	441.4091	$C_{31}H_{52}O$	-1.2	28

References

1. M. Hajji, R. Jarraya, I. Lassoued, O. Masmoudi, M. Damak and M. Nasri, *Process Biochem*, 2010, **45**, 1486-1493.
2. S. Chandra, S. Khan, B. Avula, H. Lata, M. H. Yang, M. A. Elsohly and I. A. Khan, *Evid. Based Complementary Altern. Med.*, 2014, **2014**, 253875.
3. S. Phongtongpasuk, S. Poadang and N. Yongvanich, *Energy Procedia.*, 2016, **89**, 239-247.
4. Y. Q. He, F. F. Wei, Z. Y. Ma, H. Zhang, Q. Yang, B. H. Yao, Z. R. Huang, J. Li, C. Zeng and Q. Zhang, *RSC Adv.*, 2017, **7**, 39842-39851.
5. I. L. Hsu, F. H. Yeh, Y.-C. Chin, C. I. Cheung, Z. C. Chia, L.-X. Yang, Y.-J. Chen, T.-Y. Cheng, S.-P. Wu, P.-J. Tsai, N.-Y. Lee, M.-Y. Liao and C.-C. Huang, *Chem. Eng. J.*, 2021, **409**.
6. J. K. Patra and K. H. Baek, *Front.Microbiol.*, 2017, **8**, 167.
7. S. Kaviya, J. Santhanalakshmi, B. Viswanathan, J. Muthumary and K. Srinivasan, *Spectrochim. Acta A Mol. Biomol. Spectrosc.*, 2011, **79**, 594-598.
8. G. A. Martínez-Castañón, N. Niño-Martínez, F. Martínez-Gutierrez, J. R. Martínez-Mendoza and F. Ruiz, *J Nanopart Res* . 2008, **10**, 1343-1348.
9. R. Zhao, M. Lv, Y. Li, M. Sun, W. Kong, L. Wang, S. Song, C. Fan, L. Jia, S. Qiu, Y. Sun, H. Song and R. Hao, *ACS Appl. Mater. Interfaces.*, 2017, **9**, 15328-15341.
10. A. Onodera, F. Nishiumi, K. Kakiguchi, A. Tanaka, N. Tanabe, A. Honma, K. Yayama, Y. Yoshioka, K. Nakahira, S. Yonemura, I. Yanagihara, Y. Tsutsumi and Y. Kawai, *Toxicol. Rep.*, 2015, **2**, 574-579.
11. K. Moorthy, K.-C. Chang, W.-J. Wu, J.-Y. Hsu, P.-J. Yu and C.-K. Chiang, *Nanomaterials.*, 2021, **11**.
12. S. Y. Peng, R. I. You, M. J. Lai, N. T. Lin, L. K. Chen and K. C. Chang, *Sci. Rep.*, 2017, **7**, 11477.
13. A. Nain, Y. T. Tseng, S. C. Wei, A. P. Periasamy, C. C. Huang, F. G. Tseng and H. T. Chang, *J. Hazard. Mater.*, 2020, **389**, 121821.
14. Y. Y. Loo, Y. Rukayadi, M. A. R. Nor Khaizura, C. H. Kuan, B. W. Chieng, M. Nishibuchi and S. Radu, *Front. microbiol.*, 2018, **9**.
15. F. A. Qais, A. Shafiq, H. M. Khan, F. M. Husain, R. A. Khan, B. Alenazi, A. Alsalme and I. Ahmad, *Bioinorg. Chem. Appl.*, 2019, **2019**, 4649506.
16. Y. He, F. Wei, Z. Ma, H. Zhang, Q. Yang, B. Yao, Z. Huang, J. Li, C. Zeng and Q. Zhang, *RSC Adv.*, 2017, **7**, 39842-39851.
17. E. E. Elemike, D. C. Onwudiwe, A. C. Ekennia and L. Katata-Seru, *Res. Chem. Intermed.*, 2016, **43**, 1383-1394.
18. N. D. Jasuja, D. K. Gupta, M. Reza and S. Joshi, *Braz. J. Microbiol.*, 2014, **45**, 1325-1332.
19. S. Devanesan and M. S. AlSalhi, *Int J Nanomedicine*, 2021, **16**, 3343-3356.
20. S. Sedaghat and S. Omidi, *Bioinspired Biomim. Nanobiomaterials.*, 2019, **8**, 190-197.
21. K. Li, C. Ma, T. Jian, H. Sun, L. Wang, H. Xu, W. Li, H. Su and X. Cheng, *J. Food Sci. Technol.*, 2017, **54**, 3569-3576.

22. A. K. Keshari, R. Srivastava, P. Singh, V. B. Yadav and G. Nath, *J. Ayurveda Integr. Med.*, 2020, **11**, 37-44.
23. W. R. Rolim, M. T. Pelegrino, B. de Araújo Lima, L. S. Ferraz, F. N. Costa, J. S. Bernardes, T. Rodigues, M. Brocchi and A. B. Seabra, *Appl. Surf. Sci.*, 2018, **463**, 66-74.
24. L. I. U. Rong-hua, C. Shi-sheng, R. E. N. Gang, S. Feng and H. Hui-lian, *Chin. Herb. Med.*, 2013, **5**, 240-243.
25. T. D. Xuan, T. Toyama, M. Fukuta, T. D. Khanh and S. Tawata, *J. Agric. Food Chem.*, 2009, **57**, 9448-9453.
26. A. L. Cerdeira, C. L. Cantrell, F. E. Dayan, J. D. Byrd and S. O. Duke, *Weed Sci.*, 2017, **60**, 212-218.
27. X. Liu, B. F. Zhang, L. Yang, G. X. Chou and Z. T. Wang, *Chin J Nat Medicines*, 2013, **11**, 77-80.
28. K. Nishimoto, M. Ito, S. Natori and T. Ohmoto, *Tetrahedron.*, 1968, **24**, 735-752.